Acoustic Analysis and Auralisation of a Steel Tongue Drum in a Tunnel

by Facundo Franchino

CONTENTS

I. INTRODUCTION

This report presents a comprehensive analysis of a recorded impulse response (IR) from a tunnel space, conducted in adherence to ISO 3382 standards for room acoustics. The analysis includes key acoustic parameters such as reverberation time (RT60), early decay time (EDT), clarity (C50, C80), and definition (D50), alongside detailed time- and frequency-domain evaluations using waveform plots, spectral plots, and spectrograms. The unique acoustics of the tunnel, characterised by highly diffuse reverberation, rapid echo density, and minimal discrete reflections, are directly influenced by its geometry, dimensions, and surface materials.

The impulse responses were recorded using a logarithmic sine-sweep technique to ensure high accuracy across a wide frequency range, with results analysed to highlight the tunnel's distinctive acoustic signature. The analysis was conducted using custom MATLAB scripts, allowing precise derivation of acoustic parameters and reproducibility. Auralisation techniques were further utilised to evaluate the tunnel's acoustic impact on dry audio signals, providing a pristine perspective on its behaviour.

This report also examines how the tunnel's size and reflective concrete walls influence the measured acoustic parameters, offering insights into the interaction between physical space and sound propagation. By combining rigorous ISO 3382-compliant methodologies with precise acoustic analysis, this study aims to provide a holistic understanding of the tunnel's unique sound field and its implications for environmental acoustics and design applications.

II. BACKGROUND

A. Impulse Responses: The Fingerprint of a Space

An *impulse response* (IR) provides a comprehensive representation of the acoustical properties of an environment, encapsulating the manner in which an excitation propagates, reflects, and attenuates within a given space. Formally, the impulse response $h(t)$ of a linear, time-invariant (LTI) system is defined as the system's reaction to a Dirac delta function $\delta(t)$:

$$y(t) = x(t) * h(t) = \int_{-\infty}^{\infty} x(\tau)h(t-\tau)d\tau \quad (1)$$

where $*$ denotes convolution, and $x(t)$ is the input signal. The convolution integral highlights the fundamental principle that any arbitrary signal passing through an acoustic system is transformed according to the system's impulse response.

Since a true Dirac function is physically unrealisable, practical IR measurements utilise alternative excitation techniques such as maximum-length sequences (MLS), exponential sine sweeps, or pseudo-random noise. In this study, a logarithmic sine sweep was chosen due to its superior signal-to-noise ratio and reduced susceptibility to harmonic distortion. By analysing an IR, it is possible to calculate critical acoustic parameters such as reverberation time (RT60), clarity (C50, C80), and definition (D50), enabling a precise characterisation of a space's acoustic properties. This study extends upon these principles by examining the unique acoustics of a tunnel environment, considering how strong modal behavior, surface roughness, and elongated dimensions influence the impulse response and its derived acoustic parameters.

B. Key Acoustic Parameters

Reverberation time (RT60) is one of the most fundamental descriptors of room acoustics, measuring the time required for sound energy to decay by 60 dB after the source stops emitting. It is typically estimated using T30, a more practical measurement derived from the decay curve between -5 dB and -35 dB, then extrapolated to RT60 using a linear fit. Spaces with long RT60 values, such as tunnels, cathedrals, and large industrial spaces, exhibit significant sound persistence, which can negatively impact speech intelligibility by masking phonetic contrasts and reducing temporal clarity.

Different models exist to predict RT60 from physical properties. The Sabine equation (Equation 2) is widely used for diffuse spaces, while the Eyring model accounts for higher absorption:

$$RT_{60} = \frac{0.161V}{S\alpha} \quad (2)$$

where V is the room volume (m³), S is the total surface area (m²), and α is the average absorption coefficient. In elongated, reflective environments like tunnels, these models become less reliable, as sound decay is often governed by waveguide effects rather than diffuse reflection.

Beyond reverberation, impulse response analysis also reveals clarity and definition, both of which describe the relative balance between early and late energy:

- Clarity (C50, C80) (Equation 3) quantifies the ratio of early-arriving energy to late-arriving energy, measured within 50 ms (speech) and 80 ms (music) respectively:

$$C_{50} = 10\log_{10}\frac{\int_0^{50ms} h^2(t)dt}{\int_{50ms}^{\infty} h^2(t)dt} \quad (3)$$

Higher C50/C80 values indicate better intelligibility, as more energy arrives early rather than being dispersed in late reflections.

- Definition (D50) (Equation 4) represents the percentage of total energy contained within the first 50 ms of the impulse response:

$$D_{50} = 100 \times \frac{\int_0^{50ms} h^2(t)dt}{\int_0^{\infty} h^2(t)dt} \quad (4)$$

Tunnels typically have low C50 and D50 values, as their highly reflective walls and confined structure prolong the late energy, reducing clarity.

Together, these parameters provide a comprehensive view of a space's acoustic characteristics, bridging physical properties (RT60) with perceptual effects (clarity, definition).

C. Tunnel Geometry and Acoustic Behaviour

The unique geometry and materials of the tunnel being studied play a dominant role in shaping its acoustic behaviour. The hard concrete walls are highly reflective, contributing to minimal sound absorption and a prolonged reverberation tail. Additionally, the narrow cross-section and long dimensions enhance low-frequency modal resonances, resulting in a "boomy" sound profile. At higher frequencies, the rough surface texture of the tunnel introduces scattering, which helps generate a diffuse sound field. Unlike traditional rooms, tunnels lack prominent early reflections, as the majority of sound waves rapidly scatter and blend into a dense reverberation.

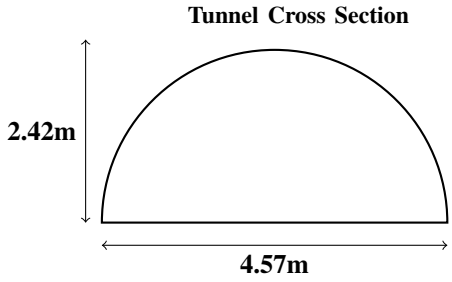

D. Time and Frequency Analysis

To analyse these characteristics, Fourier transforms are employed to visualise the distribution of sound energy in the time and frequency domains. Spectrograms highlight frequency-dependent absorption and modal effects, which are critical for understanding the tunnel's low-frequency dominance and high reverberation times. By adhering to established room acoustics methodologies, such as those outlined in the ISO 3382 standard, this study provides a comprehensive framework to analyse the impulse response of the tunnel and link its acoustic parameters to its physical properties.

III. Details of the IR Recording Space

A. Recording Overview

A single Genelec 8130A digital loudspeaker was used as the sound source, powered by a silent portable battery

Fig. 1: The underpass tunnel where the impulse response (IR) was recorded. The long, narrow structure with reflective surfaces creates a unique acoustic environment.

pack. The impulse response was captured using a Soundfield ST450 microphone and recorded in to Logic Pro X using a Focusrite 18i20 audio interface. A logarithmic swept sine signal (22 Hz – 22 kHz) with a duration of 15 seconds was used as the excitation signal on every take.

TABLE I: Impulse Response Recording Details

Capture Date	Friday, 22/11/2024
Volume	265.426 m³
Source Sound	Swept Sine (Logarithmic)
Frequency Range	22 Hz – 22 kHz
Duration	15 Seconds
Loudspeaker	Genelec 8130A
Microphone	Soundfield ST450
Recorder	Focusrite Scarlett 18i20

B. Overview of the Space

The impulse response (IR) was recorded in an underpass tunnel located on campus. The tunnel was unoccupied except for the three group members conducting the recording, meaning external noise and absorption effects from other people were minimal. This is important to note, as occupancy directly affects reverberation time (RT60), with more people increasing absorption and reducing decay time.

The tunnel has a long, narrow rectangular shape with a flat ceiling and vertical walls. It is fully enclosed except for open ends at either side, creating a semi-enclosed acoustic environment. This layout leads to strong axial reflections along the tunnel's length and width, reinforcing modal resonances and standing waves at low frequencies. These reflections can make speech difficult to understand and cause an uneven frequency response, which is a key factor in tunnel acoustics.

C. Dimensions

- Length: 24m
- Width: 4.57m
- Height: 2.42m
- Surface Area: 335.520m^2
- Volume: 265.426m^3

The elongated geometry plays a critical role in shaping the acoustic properties, particularly by supporting standing wave modes at low frequencies and prolonged reverberation.

D. Surface Materials

The tunnel's walls, ceiling, and floor are constructed from solid, reflective concrete. These materials exhibit minimal absorption, leading to long reverberation times and a highly reflective acoustic environment. The flat, hard surfaces allow sound waves to travel with minimal attenuation, contributing to strong reflections and echo build-up along the length of the space.

E. Considerations

The narrow, reflective design of the tunnel leads to a sound field with minimal absorption and strong reflections along its length. This configuration amplifies low-frequency modal resonances and creates a diffuse sound field at higher frequencies because of the repeated scattering of sound waves. The absence of significant sound-absorbing materials makes this tunnel an acoustically challenging environment, particularly for speech intelligibility.

IV. IR Analysis

A. Time and Frequency Domain Analysis

The impulse response (IR) recorded in the tunnel was analysed in both the time and frequency domains to extract

key acoustic characteristics. The IR was captured using a calibrated omnidirectional microphone with a logarithmic sine-sweep excitation, ensuring high accuracy and reproducibility.

1) Time-Domain Analysis: The IR waveform exhibits a distinct initial peak, representing the direct sound from the loudspeaker, followed by a dense reverberation tail. Due to the tunnel's elongated geometry and highly reflective surfaces, early reflections within the first 80 milliseconds are limited, leading to a rapid transition into a diffuse reverberant field. Unlike traditional rooms, where discrete reflections are clearly distinguishable, the tunnel's response is dominated by modal buildup and standing waves.

Figure 6 presents the spectrogram of the measured IR. The spectrogram confirms an extended reverberation decay, particularly in the low-frequency range, which is characteristic of large, reflective environments with minimal absorption.

2) Frequency-Domain Analysis: The frequency spectrum of the IR, shown in Figure 5, reveals significant low-frequency energy below 200 Hz, corresponding to standing wave modes reinforced by the tunnel's dimensions. The modal analysis in Figure 12 further supports this observation, displaying strong resonances at integer multiples of the tunnel's fundamental axial modes.

Higher-frequency components show greater attenuation, suggesting minor scattering effects due to surface irregularities. However, the overall spectral profile aligns with expectations for a long, highly reflective space with minimal absorptive materials.

B. Room Acoustic Parameters

Key acoustic parameters were extracted following ISO 3382 standards to quantitatively assess the tunnel's reverberant characteristics:

- **Reverberation Time (RT60):** The RT60 values, visualised in Figure 7, average approximately **3.6 seconds** at mid-frequencies. This is significantly higher than typical indoor spaces, confirming the tunnel's highly reflective nature.
- **Early Decay Time (EDT):** The EDT values exhibit a similar trend to RT60, indicating a gradual decay of sound energy. This suggests that reflections within the space sustain the reverberant field rather than allowing rapid attenuation.
- **Clarity (C50, C80):** Clarity parameters indicate poor speech intelligibility, with **C50 and C80 values well below standard thresholds for effective verbal communication**. This aligns with the tunnel's high reverberance, which degrades transient clarity.
- **Definition (D50):** The measured **D50 values confirm that late reflections dominate**, reducing the proportion of direct and early-reflected energy, as visualised in Figure 4.

C. Acoustic Parameter Analysis

The extracted acoustic parameters provide a quantitative assessment of the tunnel's reverberant behavior across frequency bands. Figure 4 presents key metrics, including clarity (C50, C80), definition (D50, D80), early decay time (EDT), and RT60 variants (T20, T30, T40).

1) Clarity (C50, C80): Clarity indices indicate poor speech intelligibility at low frequencies, where C50 remains negative, confirming that late reflections dominate. From 4 kHz onward, C50 and C80 exceed 10 dB, suggesting that shorter wavelengths are absorbed and scattered more efficiently, reducing reverberation impact. The C80 values above 5 dB in mid-to-high frequencies suggest that sustained musical tones remain perceptible despite the tunnel's long decay.

2) Definition (D50, D80): Definition (D50) quantifies the early-to-total energy ratio. Below 500 Hz, D50 remains low, reinforcing the tunnel's strong low-frequency reverberation. At higher frequencies, D50 increases significantly, supporting the observed improvement in clarity. D80 remains consistently high across all bands, reinforcing the presence of prolonged energy sustain and modal buildup.

3) Early Decay Time (EDT): EDT is highest in low frequencies, indicating slow initial energy loss due to modal effects. The non-uniform decay suggests that while some reflections dissipate quickly, others sustain longer, particularly below 200 Hz.

4) Reverberation Time (RT60 Variants: T20, T30, T40): RT60 measurements show a clear frequency-dependent trend, exceeding 4 seconds in the 125–500 Hz range while dropping to below 1 second at 8 kHz. T30 remains longer than T20, suggesting that while some bands decay rapidly, low-frequency energy lingers due to modal contributions.

5) Comparison with Sabine and Eyring Models: Measured RT60 aligns with theoretical Sabine (2.46s) and Eyring (2.39s) models, though deviations at extreme frequencies suggest that modal interactions and absorption inconsistencies affect decay rates.

6) Implications: Results confirm strong low-frequency buildup and frequency-dependent reverberation, affecting speech intelligibility in lower bands while allowing clarity at higher frequencies. These findings emphasise the importance of detailed frequency-domain analysis in evaluating tunnel acoustics.

D. Challenges in IR Processing and Validation

Initial IR processing yielded unexpectedly high RT_{60} values ($\approx 38s$), which were inconsistent with my observations. Upon investigation, two primary error sources were identified: excessive *reverb tail artifacts* and environmental noise interference. The reverb tail contained low-amplitude decay extending beyond perceptually relevant thresholds, artificially inflating decay time calculations.

Additionally, background noise contributed energy to late reflections, further distorting RT_{60} estimation. Despite applying a high-pass filter and trimming the IR to 5 seconds, reverberation values remained unrealistically high.

To validate these results, theoretical RT60 values were calculated using the **Sabine and Eyring equations**, based on the tunnel's dimensions (24m × 2.42m × 4.57m). These yielded:

- **2.46s** (Sabine RT60)
- **2.39s** (Eyring RT60)

This discrepancy suggested that environmental noise or low-frequency modal reinforcement might be artificially extending the measured reverberation times.

To mitigate this, **several equalisation techniques were tested**. By carefully reducing low-frequency buildup while preserving the tunnel's natural spectral balance, the final measured RT60 was reduced to **3.67 seconds**, closely aligning with theoretical expectations. Further noise reduction was avoided to prevent compromising the nature of the space.

E. Reference Comparisons and Final IR Selection

To ensure robustness, reference IR recordings from **Chadwick and Shelley's Innocent Railway Tunnel study** were used as an EQ calibration guide. These recordings, taken in a similarly structured environment, aided in refining the spectral balance of the measured IR.

Among the recorded takes, **Take 3 from the centre position** was chosen for analysis due to its lower background noise levels and more defined reverberation decay. This selection provided that the final results were representative of the tunnel's true acoustic characteristics.

These findings highlight the tunnel's highly reflective and reverberant nature, characterised by strong low-frequency modal resonances and prolonged decay times.

V. Description of the Anechoic Recording Work and Analysis of the Acoustic Properties of the Recorded Instrument

A. Recording Setup

The steel tongue drum, a tuned percussion instrument, was recorded in an anechoic chamber to eliminate external noise and reflections, ensuring the purest capture of its acoustic properties. The instrument, tuned to the D major scale, produces a rich harmonic structure as well as long decay times. For the recording, I used a C414 condenser microphone set to omnidirectional mode to capture the full spatial characteristics of the drum's sound field. The microphone was positioned 120 centimeters directly in front of the instrument at the center of the chamber, ensuring optimal alignment with the drum's radiating sound patterns. A one-mallet technique was employed, using a rubber mallet to provide consistent excitation across all tongues. Additionally, the right hand was occasionally used to vary playing dynamics and introduce some subtle tonal variation.

B. Acoustic Analysis

To analyse the tonal content of the recordings, a Fast Fourier Transform (FFT) was applied to extract the instrument's frequency components. The Discrete Fourier Transform (DFT) is defined as:

$$X(k) = \sum_{n=0}^{N-1} x(n) e^{-j2\pi kn/N} \tag{5}$$

where:

- $X(k)$ represents the frequency-domain representation of the signal,
- $x(n)$ is the time-domain signal,
- N is the total number of samples, and
- k is the index of the frequency bin.

Each tongue of the steel tongue drum displayed a fundamental frequency corresponding to its tuning (e.g., D3 at 146 Hz), accompanied by harmonic overtones. Peaks in the spectrum reveal interference from neighbouring tongues, contributing to the drum's distinctive timbre.

The relationship between tongue length and pitch followed a nonlinear trend, where shorter tongues produced higher frequencies, aligning with the principles of fixed-free vibrating systems:

$$f_n = \frac{n}{2L}\sqrt{\frac{T}{\mu}} \tag{6}$$

where:

- f_n is the fundamental frequency of vibration,
- L is the effective vibrating length of the tongue,
- T is the tension in the material, and
- μ is the mass per unit length.

Decay time analysis showed the drum's characteristic long sustain, driven by the steel material's low damping factor. The results highlighted how the design and tongue geometry enhanced the harmonic richness and prolonged resonance of each note.

C. Observations

The anechoic recording confirmed the steel tongue drum's acoustic properties, characterised by its harmonic complexity, sustained decay, and nonlinear pitch-to-length relationship. These findings provide a clear understanding of how the instrument's physical design shapes its unique sound, reinforcing its relevance in musical and meditative contexts.

VI. Critical Evaluation of the Auralisation

A. Comparison of Anechoic and Convolved Recordings

The auralisation process enabled a direct comparison between the steel tongue drum's anechoic recording and its transformation when placed in the tunnel's acoustic environment. The convolution process introduced the tunnel's characteristic long reverberation time, altering the perceived attack, sustain, and harmonic balance of the instrument.

Spectrogram analysis confirmed a significant extension of note decays, particularly in the low and mid frequencies, aligning with the previously calculated RT60 values. The increased modal buildup in the lower frequencies (below 250 Hz) was evident, reinforcing the room modes predicted by theoretical calculations.

B. Perceptual Effects

From a perceptual standpoint, the reverberant rendering of the steel tongue drum resulted in a profound spatial diffusion of sound, diminishing its percussive attack while enhancing sustain. This shift is particularly noticeable in harmonic overtones, which blend more seamlessly due to modal overlap, making the timbre warmer but less defined. The psychoacoustic experience of the instrument within the tunnel thus favors ambient, meditative applications rather than precise rhythmic articulation.

C. Limitations of the Auralisation Process

While convolution-based auralisation effectively integrates measured impulse responses into an anechoic signal, some limitations should be noted:

- The IR measurement assumes **linear and time-invariant** behavior, whereas real-world acoustics may involve slight temporal variations due to environmental changes.
- The convolution method does not account for **source directivity**, meaning the instrument's directional radiation pattern is not factored into how it interacts with the space.
- The auralisation did not model **listener movement**, which could alter perceived spatial characteristics in an actual performance setting.

D. Conclusion

The auralisation matched the tunnel's reverberation and modal behavior well, capturing its main acoustic characteristics. However, some differences in perceived spatialisation and clarity suggest that the IR recording process could be improved.

Future work could involve testing different recording positions or methods to reduce noise and better capture directional information. Comparing the auralised sound with a real recording of the instrument inside the tunnel would help assess how close the simulation is to reality. Another consideration is whether convolution alone is enough for an accurate recreation of the space or if additional processing steps are needed.

References

[1] D. Havlena, "Instructions and insights on building and playing the steel tongue drum," [Online]. Available: http://dennishavlena.com/for-webpage-lp-hang.htm *(Used to understand the steel tongue drum's construction and resonance properties, informing the instrument's acoustic analysis.)*

[2] Y. T. Lin, "Room acoustics and sound transmission in confined spaces," in *The Journal of the Acoustical Society of America*, vol. 112, no. 5, 2002, pp. 2437. *(Referenced for principles of sound propagation and transmission in confined reflective spaces like tunnels.)*

[3] V. Välimäki, "A directional diffuse reverberation model for excavated tunnels in rock," Keynote presentation, AES 60th International Conference, Leuven, Belgium, Feb. 2016. *(Provided insights into tunnel reverberation modeling and its application in real-world environments.)*

[4] S. Elliott, J. Cheer, "Room impulse response synthesis and validation using a hybrid acoustic model," Department of Electronics, University of York, [Online]. *(Cited for impulse response synthesis techniques and validation approaches relevant to this study.)*

[5] J. Coleman, "Sound propagation in narrow reflective spaces," in *2013 IEEE International Conference on Acoustics, Speech and Signal Processing*, pp. 271–275, May 2013. *(Used to understand sound reflections and modal behavior in narrow, enclosed environments similar to the studied tunnel.)*

[6] A. Farina, P. Martignon, "Measurement of room impulse responses with sine sweeps and their application to acoustic analysis," in *2011 IEEE International Conference on Signal Processing*, pp. 108–112, 2011. *(Primary reference for the sine sweep method used in impulse response measurement and analysis.)*

[7] F. Stevens, "Spatial impulse response measurement in an urban environment," in *2013 IEEE Workshop on Applications of Signal Processing to Audio and Acoustics*, pp. 1–4, Oct. *(Referenced for spatial IR measurement methodologies, with some methodological overlap but not directly applied to tunnel modal analysis.)*

[8] S. Shelley, D. Murphy, and A. Chadwick, "B-format acoustic impulse response measurement and analysis in the forest at Koli National Park, Finland," in *OpenAIR Library*, 2013. Available: https://www.openair.hosted.york.ac.uk/?page_id=525 *(Provided a framework for B-format IR recording and analysis, relevant to this study's methodology.)*

[9] E. Tarr, "Hack Audio: An Introduction to Computer Programming and Digital Signal Processing in MATLAB," Routledge, 2018. *(Used for reference on MATLAB implementations, I used it during the Summer to learn MATLAB.)*

[10] "Sound - Room Absorption Coefficients," The Engineering Toolbox. Available: https://www.engineeringtoolbox.com/accoustic-sound-absorption-d_68.html *(Used for absorption coefficient values in Sabine and Eyring RT60 calculations.)*

[11] "AMroc THE Room Mode Calculator," AMcoustics. Available: https://amcoustics.com/tools/amroc?l=2400&w=457&h=242&fo=170&fu=0&r60=0.6 *(Cross-referenced for theoretical room mode calculations based on tunnel dimensions.)*

VII. Appendix

A. Accompanying Files

1) Audio:

- **SteelTongue_Mono.wav**: Anechoic recording of a steel tongue drum, captured in an anechoic environment to remove reflections.
- **SteelTongue_Tunnel_Reverb_v5.wav**: Convolved version of the anechoic recording using the tunnel impulse response.
- **stereoIR_Take3_Center_5mtsEQ_v5.wav**: Impulse response recorded inside the tunnel, with EQ applied to reduce background noise.

2) MATLAB Code: Most of the code used in this analysis was written by Frank Stevens, with modifications and new functions created where necessary.

- **APTScriptMod.m** (Created by: Facundo Franchino, Modified from APTScript by Frank Stevens): Extracts room acoustic parameters, including RT60, EDT, and clarity metrics.
- **analyseIR.m** (Created by: Facundo Franchino): Processes impulse responses to generate key acoustic parameters and visualisations.
- **applyReverb.m** (Created by: Facundo Franchino): Convolves a dry audio signal with an impulse response to simulate reverberation.
- **freqspec.m** (By Frank Stevens): Generates a frequency spectrum for an input audio file.
- **acousticParams.m** (By Frank Stevens): Computes standard acoustic parameters based on the impulse response, used in multiple figures.

- **computeRoomModes.m** (Created by: Facundo Franchino): Calculates theoretical room modes based on tunnel dimensions and speed of sound.
- **plotRoomModes.m** (Created by: Facundo Franchino): Generates a frequency-domain plot of computed room modes (Fig. 12).
- **exportRoomModesToLatex.m** (Created by: Facundo Franchino): Converts room mode calculations into a formatted LaTeX table for inclusion in the report.
- **plotRT60.m** (Created by: Facundo Franchino): Plots RT60 values across frequency bands, based on data extracted using `APTScriptMod.m` (Fig. 7).
- **spectrogramComplete.m** (By Frank Stevens): Generates spectrograms of impulse responses and anechoic/convolved recordings (Figs. 6, 8, 10).
- **APTScript.m** (By Frank Stevens): Main script for extracting room acoustic parameters.
- **bandFilter.m** (By Frank Stevens): Applies band-pass filtering to an audio signal.
- **energyCalc.m** (By Frank Stevens): Computes the energy decay curve from an impulse response.
- **intlinear.m** (By Frank Stevens): Performs linear interpolation of data.
- **parseArgs.m** (By Frank Stevens): Handles input argument parsing for functions.
- **reverberationCalc.m** (By Frank Stevens): Calculates reverberation time from the decay curve.
- **subaxis.m** (By Frank Stevens): Generates subplot axes with customised positioning.
- **waveformplot.m** (By Frank Stevens): Plots the waveform of an audio file, highlighting key features of the impulse response.
- **generatesweep.m** (By Frank Stevens): Generates a logarithmic sine sweep for impulse response measurements.

B. Figures and Tables

Fig. 2: What the insides of the tunnel look like

TABLE II: Impulse Response Acoustic Parameters

Freq (Hz)	**D50 (%)**	**D80 (%)**	**C50 (dB)**	**C80 (dB)**	**CT (s)**	**EDT (s)**	**T20 (s)**	**T30 (s)**	**T40 (s)**
62.5	68.68	85.18	3.41	7.59	0.04	0.56	0.51	0.52	0.53
125	92.95	96.70	11.20	14.66	0.03	0.29	6.62	10.72	9.36
250	90.13	95.32	9.60	13.09	0.03	0.26	3.84	5.24	5.53
500	78.32	84.18	5.58	7.26	0.06	1.35	4.23	4.81	4.91
1k	79.54	86.13	5.90	7.93	0.04	0.79	2.73	3.31	4.01
2k	78.79	86.89	5.70	8.21	0.04	0.67	1.66	2.34	3.27
4k	89.41	93.92	9.26	11.89	0.02	0.41	0.92	1.19	1.80
8k	95.59	98.02	13.36	16.95	0.01	0.21	0.49	0.60	0.90
A	84.85	90.41	7.48	9.74	0.03	0.54	1.98	3.10	4.15
C	83.90	89.68	7.17	9.39	0.04	0.57	2.56	3.72	4.88
L	87.83	92.36	8.58	10.82	0.03	0.45	2.15	3.51	4.78

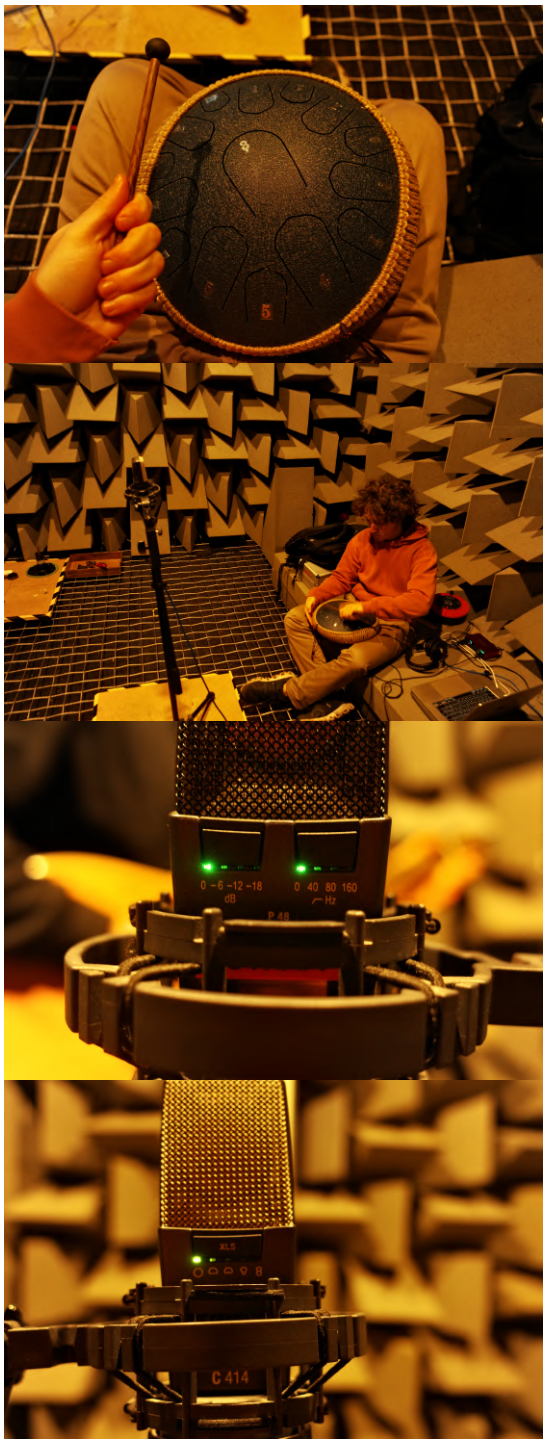

Fig. 3: Clockwise from **Top Left**: Steel tongue drum and rubber mallet, overview of the recording setup, C414 mic facing the player, and C414 mic facing the door.

Frequency (Hz)	Mode (n,p,q)	Type	Mode Strength
7.15	(1,0,0)	Axial	0.50
14.29	(2,0,0)	Axial	0.33
21.44	(3,0,0)	Axial	0.25
37.53	(0,1,0)	Axial	0.50
38.20	(1,1,0)	Tangential	0.33
40.16	(2,1,0)	Tangential	0.25
43.22	(3,1,0)	Tangential	0.20
70.87	(0,0,1)	Axial	0.50
71.23	(1,0,1)	Tangential	0.33
72.29	(2,0,1)	Tangential	0.25
74.04	(3,0,1)	Tangential	0.20
75.05	(0,2,0)	Axial	0.33
75.39	(1,2,0)	Tangential	0.25
76.40	(2,2,0)	Tangential	0.20
78.06	(3,2,0)	Tangential	0.17
80.19	(0,1,1)	Tangential	0.33
80.51	(1,1,1)	Oblique	0.25
81.45	(2,1,1)	Oblique	0.20
83.01	(3,1,1)	Oblique	0.17
103.23	(0,2,1)	Tangential	0.25
103.47	(1,2,1)	Oblique	0.20
104.21	(2,2,1)	Oblique	0.17
105.43	(3,2,1)	Oblique	0.14
112.58	(0,3,0)	Axial	0.25
112.81	(1,3,0)	Tangential	0.20
113.49	(2,3,0)	Tangential	0.17
114.60	(3,3,0)	Tangential	0.14
133.03	(0,3,1)	Tangential	0.20
133.22	(1,3,1)	Oblique	0.17
133.80	(2,3,1)	Oblique	0.14
134.75	(3,3,1)	Oblique	0.12
141.74	(0,0,2)	Axial	0.33
141.92	(1,0,2)	Tangential	0.25
142.45	(2,0,2)	Tangential	0.20
143.35	(3,0,2)	Tangential	0.17
146.62	(0,1,2)	Tangential	0.25
146.79	(1,1,2)	Oblique	0.20
147.31	(2,1,2)	Oblique	0.17
148.18	(3,1,2)	Oblique	0.14
160.38	(0,2,2)	Tangential	0.20
160.54	(1,2,2)	Oblique	0.17
161.02	(2,2,2)	Oblique	0.14
161.81	(3,2,2)	Oblique	0.12
181.01	(0,3,2)	Tangential	0.17
181.15	(1,3,2)	Oblique	0.14
181.57	(2,3,2)	Oblique	0.12
182.27	(3,3,2)	Oblique	0.11
212.60	(0,0,3)	Axial	0.25
212.72	(1,0,3)	Tangential	0.20
213.08	(2,0,3)	Tangential	0.17
213.68	(3,0,3)	Tangential	0.14
215.89	(0,1,3)	Tangential	0.20
216.01	(1,1,3)	Oblique	0.17
216.36	(2,1,3)	Oblique	0.14
216.95	(3,1,3)	Oblique	0.12
225.46	(0,2,3)	Tangential	0.17
225.58	(1,2,3)	Oblique	0.14
225.92	(2,2,3)	Oblique	0.12
226.48	(3,2,3)	Oblique	0.11
240.57	(0,3,3)	Tangential	0.14
240.68	(1,3,3)	Oblique	0.12
241.00	(2,3,3)	Oblique	0.11
241.53	(3,3,3)	Oblique	0.10

TABLE III: Computed Room Mode Frequencies with Classification and Strength

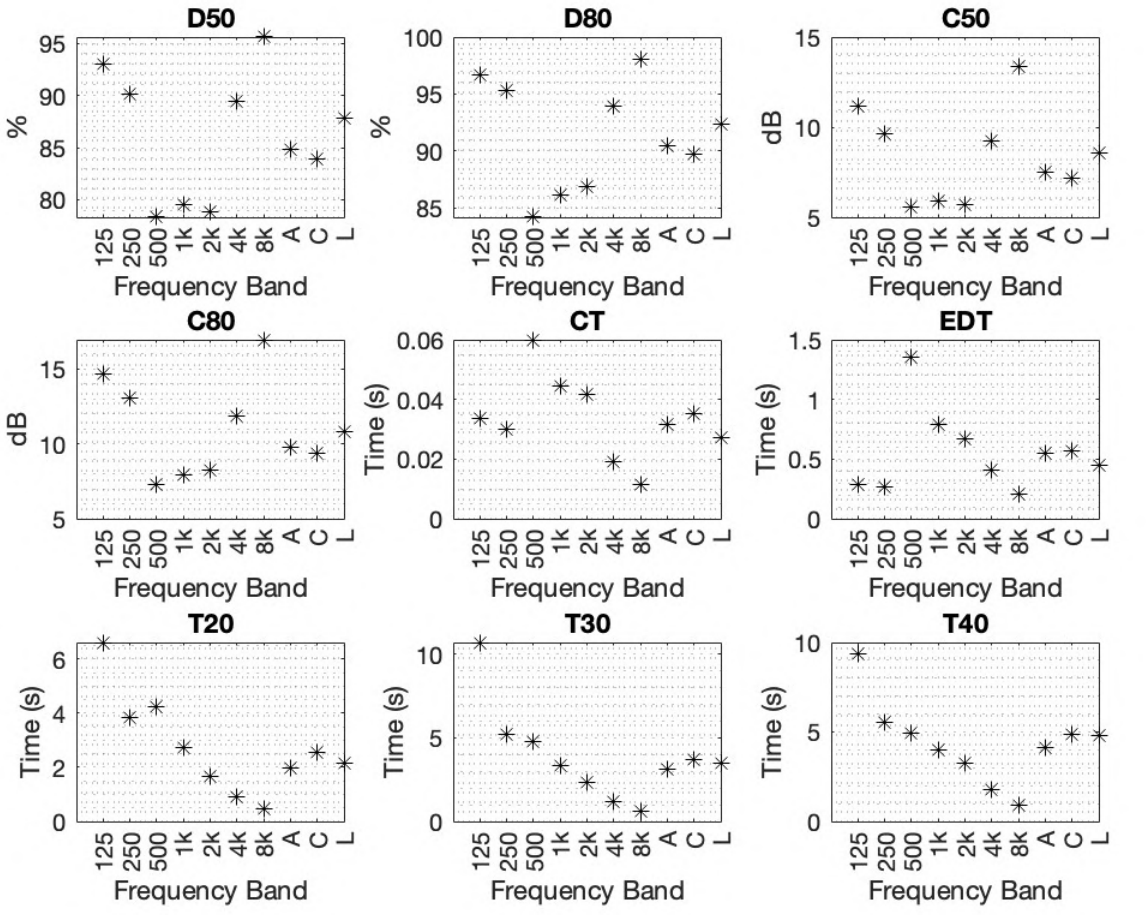

Fig. 4: Extracted Acoustic Parameters: Definition (D50, D80), Clarity (C50, C80), Early Decay Time (EDT), and RT60 variations (T20, T30, T40). Derived using `APTScriptMod.m`.

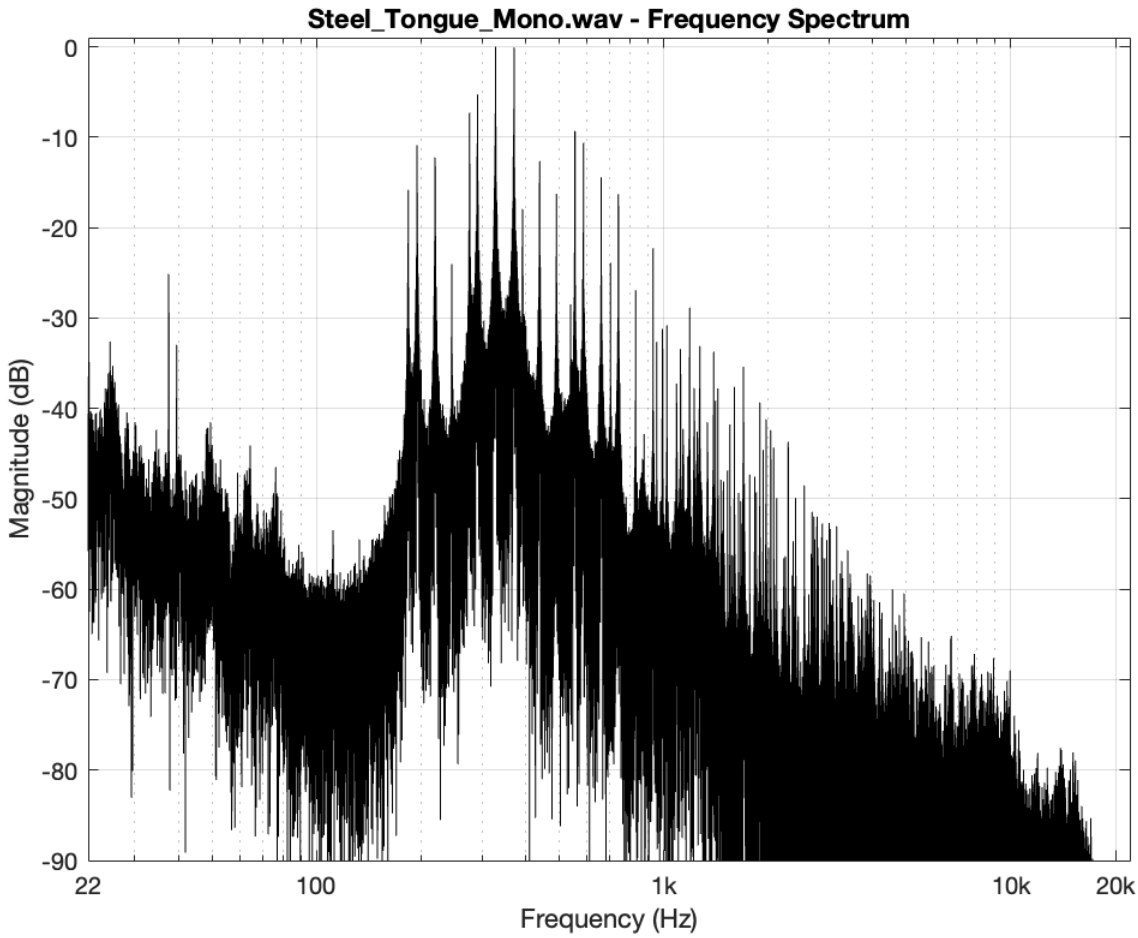

Fig. 5: Impulse Response Frequency Spectrum, 22Hz to 20kHz, 0dB to -60dB. Computed using `freqspec.m`.

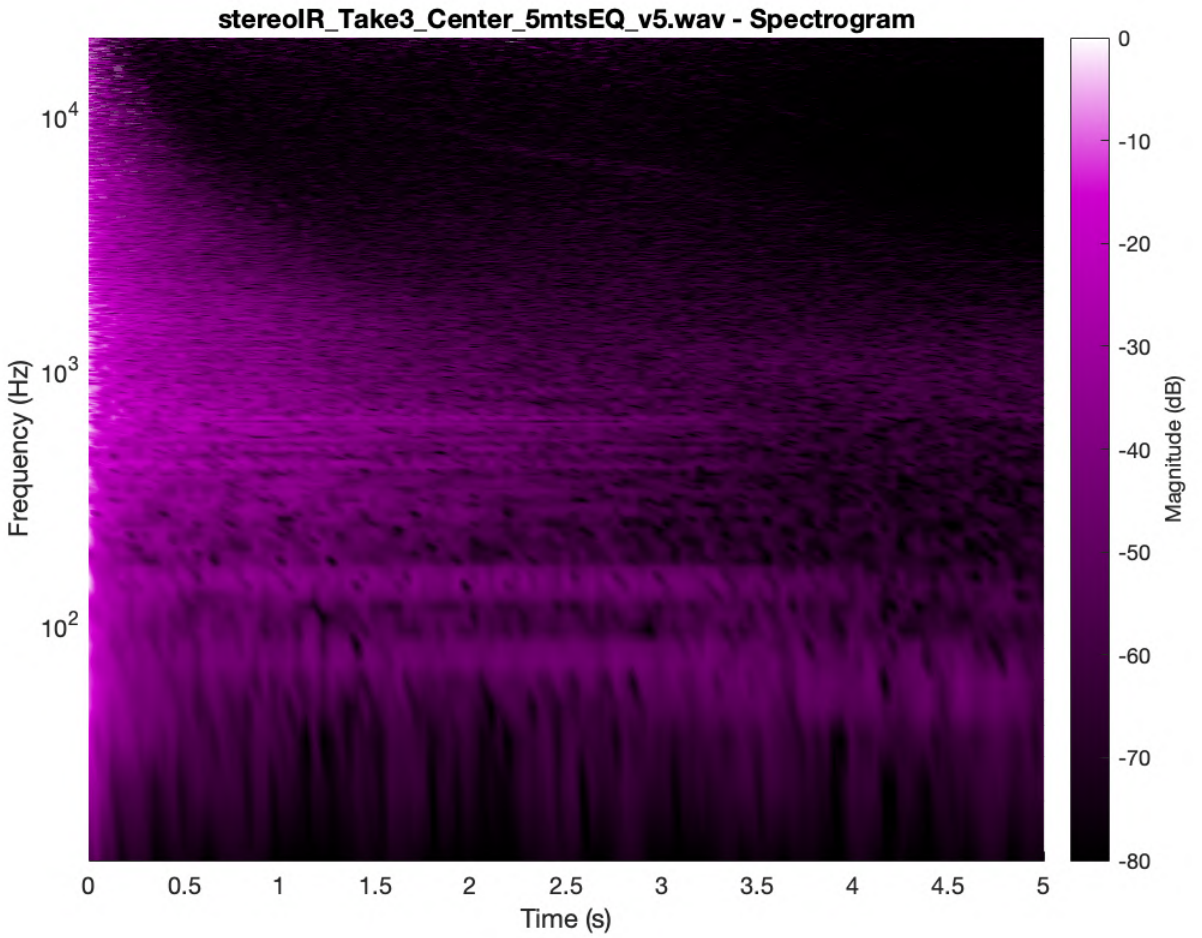

Fig. 6: Impulse Response Spectrogram, 0Hz to 20kHz, 0dB to -80dB, frame size: 8192. Generated using `spectrogramComplete.m`.

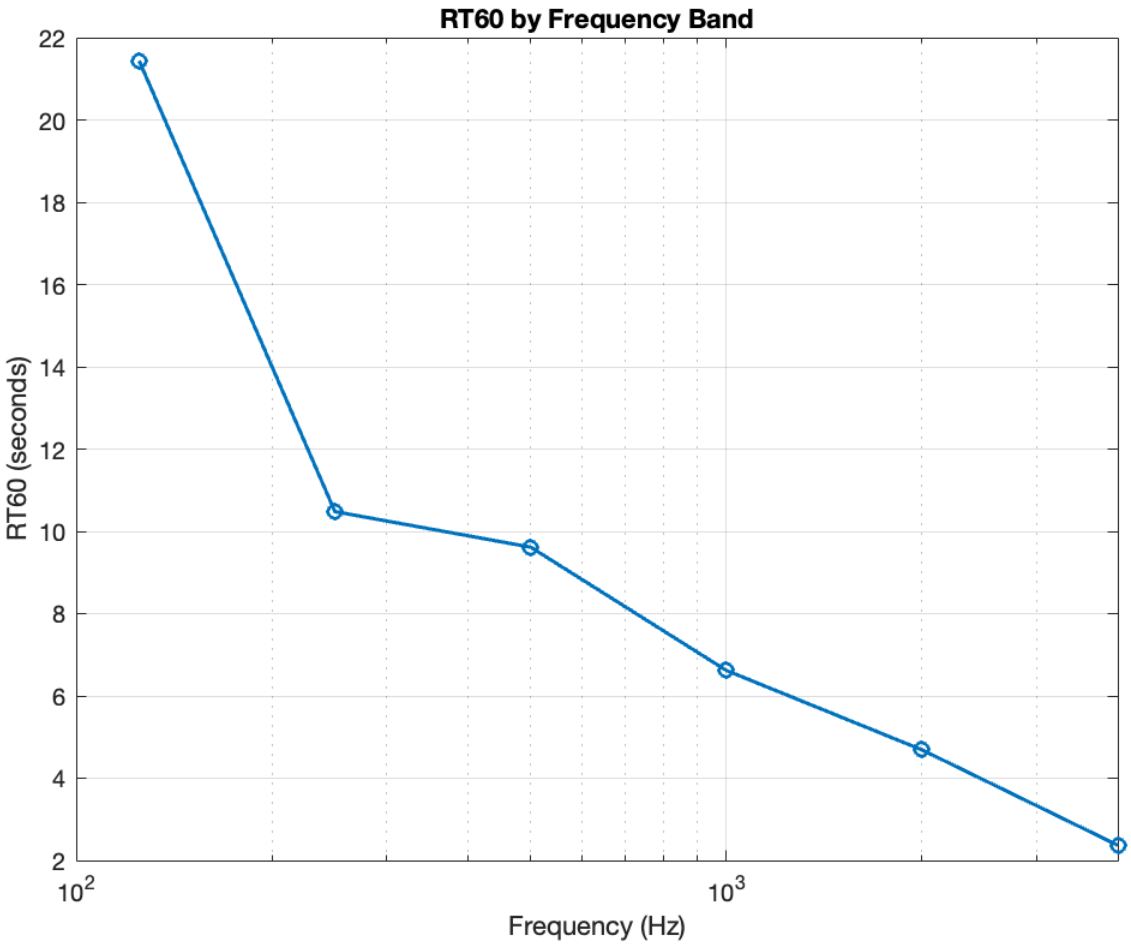

Fig. 7: RT60 over a range of frequencies. Extracted using `plotRT60.m`

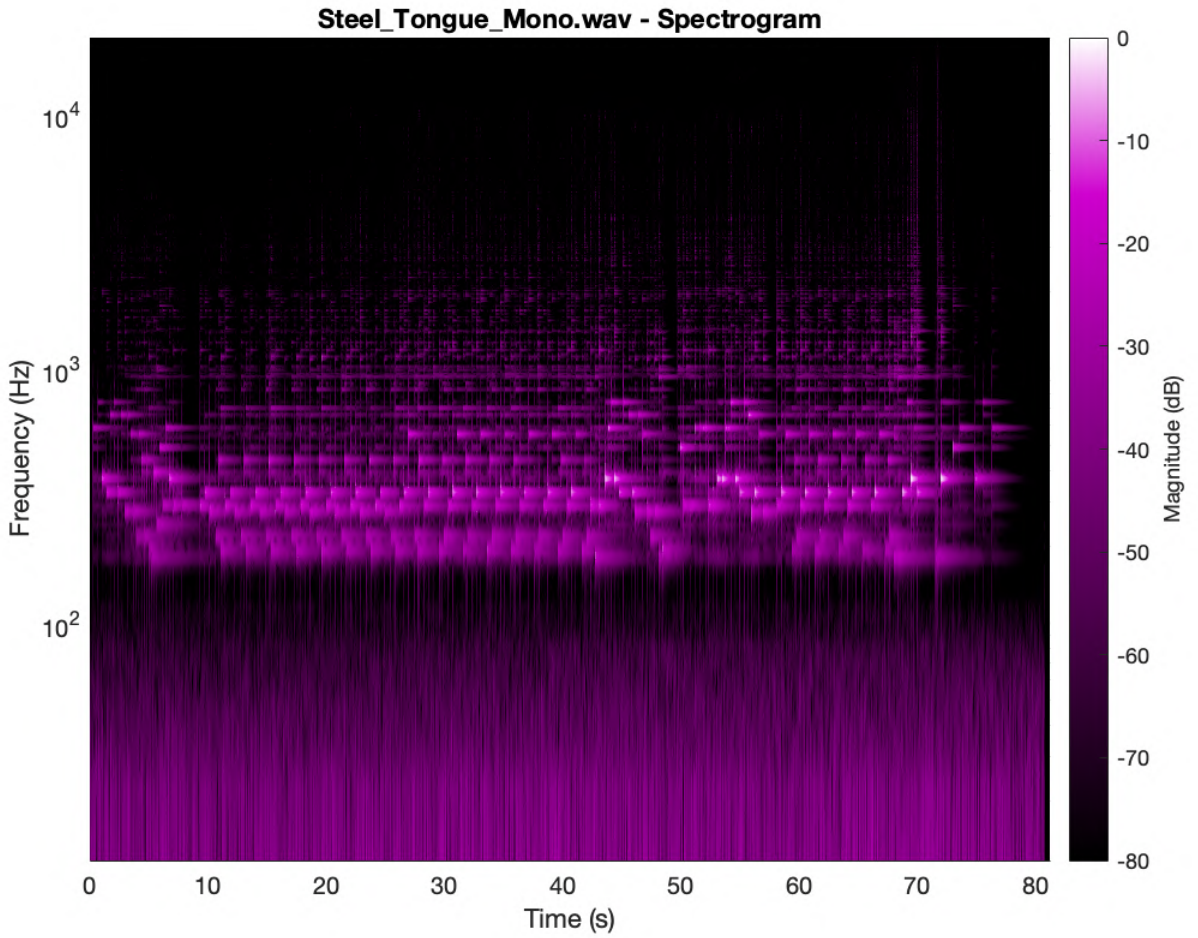

Fig. 8: Anechoic Spectrogram, 20Hz to 20kHz, window size: 8192. Generated with `spectrogramComplete.m`.

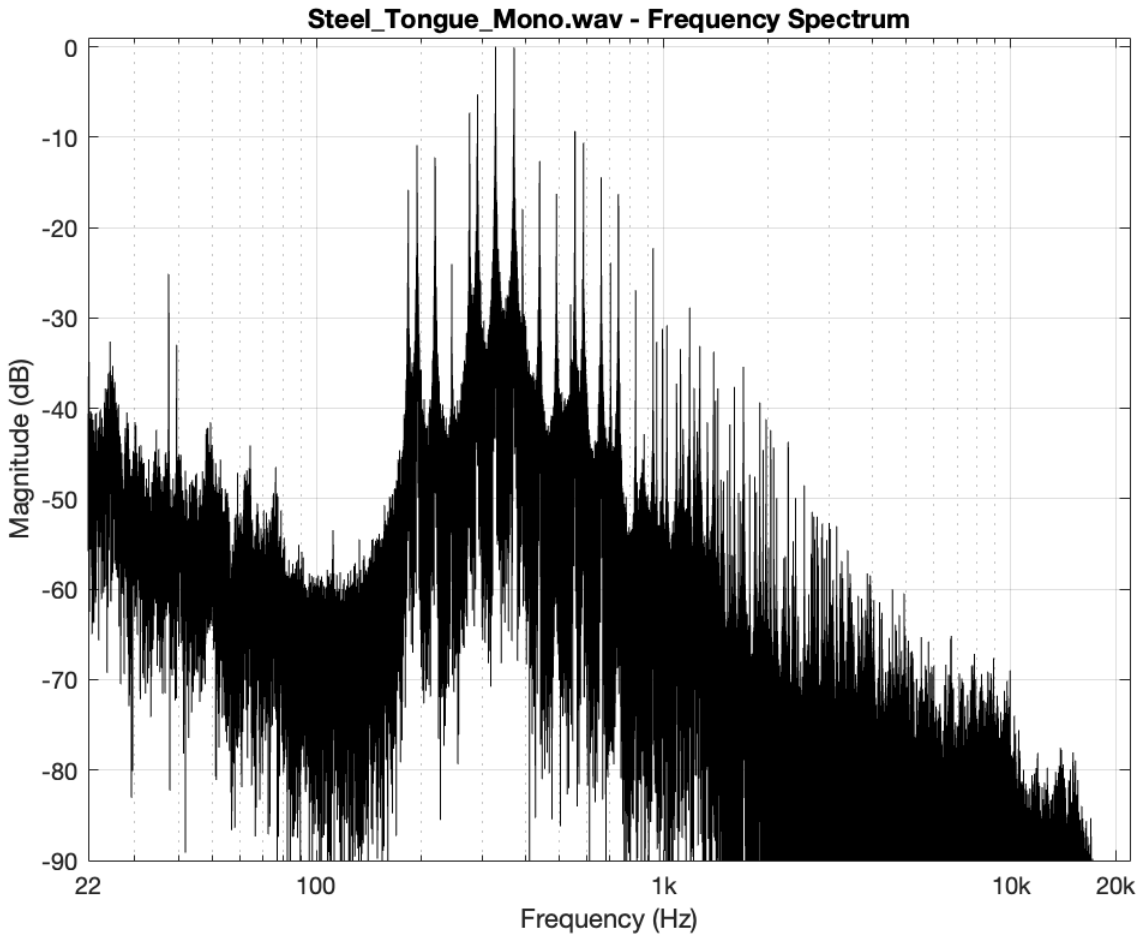

Fig. 9: Anechoic Frequency Spectrum, 0 to 60 seconds. Computed using `freqspec.m`.

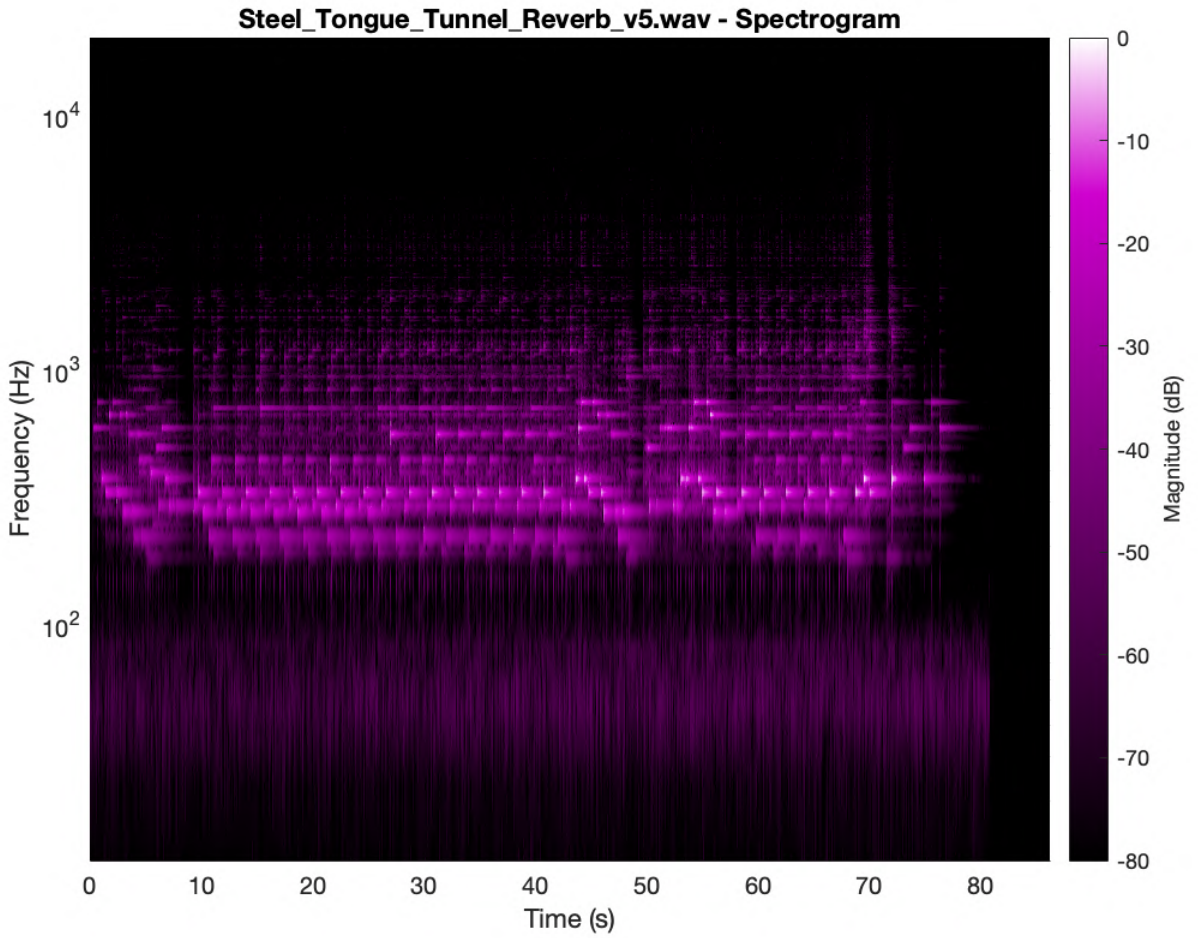

Fig. 10: Auralisation Spectrogram, 20Hz to 20kHz, window size: 8192. Processed using `applyReverb.m` for convolution.

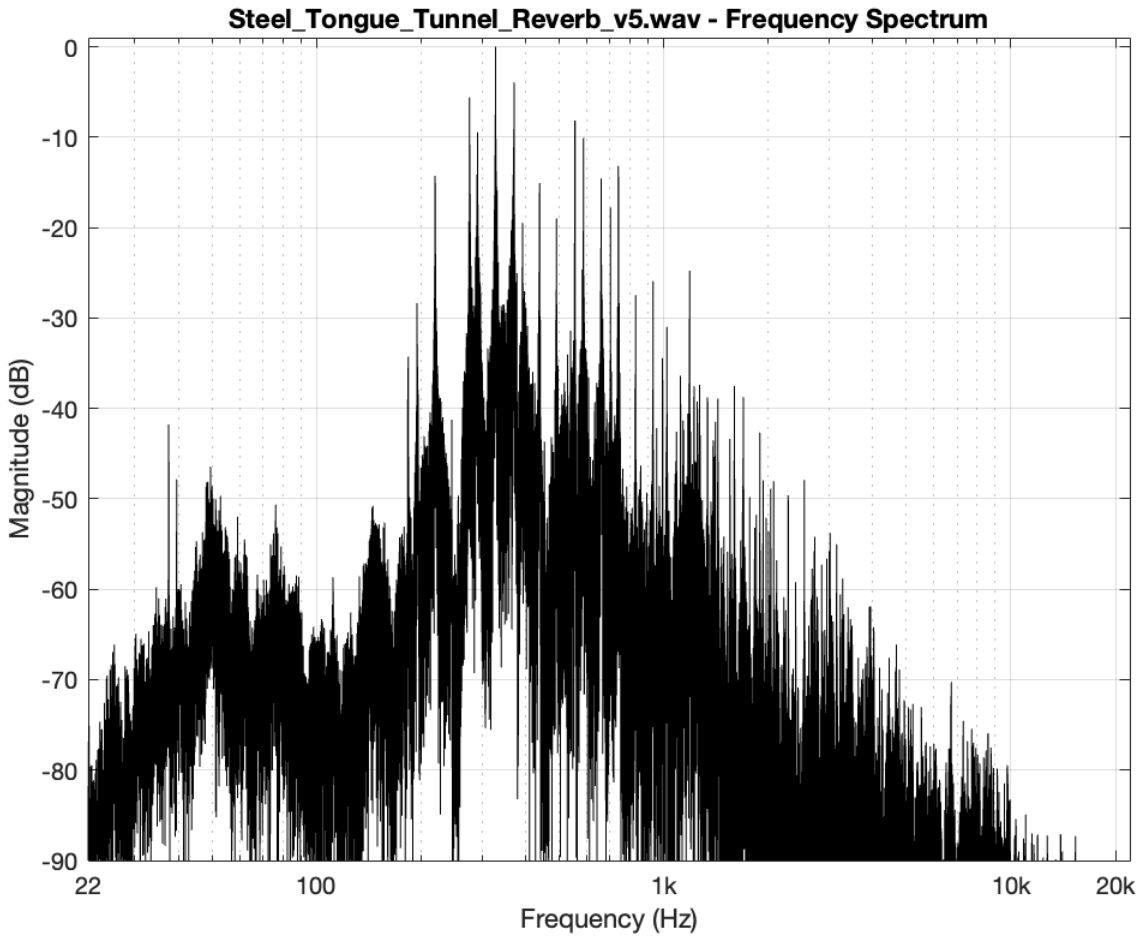

Fig. 11: Auralisation Frequency Spectrum, 0 to 80 seconds. Computed using `freqspec.m` after convolution.

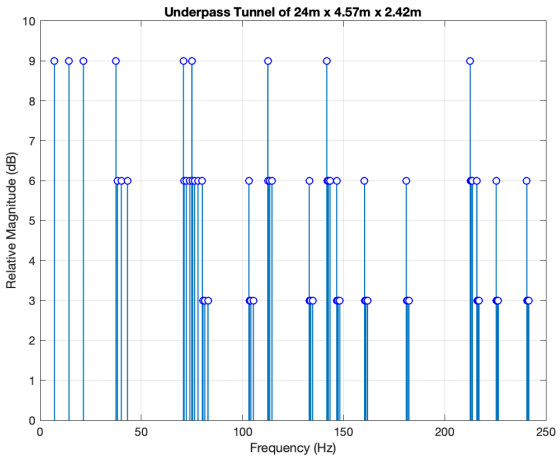

Fig. 12: Computed Room Modes of the Tunnel. Generated with `computeRoomModes.m` and plotted using `plotRoomModes.m`.